Available online at www.sciencedirect.com

SCIENCE DIRECT®

Continental Shelf Research 26 (2006) 589–598

CONTINENTAL SHELF RESEARCH

www.elsevier.com/locate/csr

A numerical and field study on inner-surf and swash sediment transport

Tian-Jian Hsu[a,*], Britt Raubenheimer[b]

[a]Department of Civil and Coastal Engineering, University of Florida, Gainesville, FL 32611, USA
[b]Applied Ocean Physics and Engineering, Woods Hole Oceanographic Institution, Woods Hole, MA 02189, USA

Received 31 January 2005; received in revised form 18 July 2005
Available online 22 March 2006

Abstract

Field observations and numerical model simulations are used to investigate mechanisms of sediment transport in the inner-surf and swash zones. Both the detailed two-phase and (dilute) turbulent suspension model results suggest that sediment transport is in phase with the bottom stress and can be parameterized by a Meyer–Peter-type power law for typical sandy-beach grain sizes ($0.2 \leqslant$ diameter $\leqslant 0.5$ mm) and wave conditions (wave period $\geqslant 5$ s). However, comparison of bottom stress (and the resulting sediment transport) predicted from observed flows by the detailed models with that predicted by a quasi-steady model suggests that the phase lag between the bottom stress and the fluid forcing may be important under strongly pitched-forward, saw-tooth-shaped swell and sea waves. Bottom stress predicted by a boundary-layer model that accounts for flow turbulence, but not particle interactions, is similar to that from the two-phase model if a large roughness is used to compensate for neglected intergranular and fluid–sediment interactions. Preliminary analysis of field observations in the swash zone suggests that breaking-wave (surface) generated turbulence affects the near-bed flow during passage of the breaking wave (bore) front and may have significant effects on sediment transport.

Keywords: Sediment transport; Surf zone; Swash zone; Bottom stress; Breaking wave turbulence

1. Introduction

Sediment exchange between the swash zone, the region of the beach that alternately is covered and uncovered by waves, and the surf zone is important to shoreline evolution. For example, it has been suggested (List et al., 2003) that the observed storm-driven erosion and post-storm accretion at erosional hot spots (List and Farris, 1999) may be owing to cross-shore movement of sediment between the swash and inner-surf zones, which may be largest in locations not protected by multiple offshore sandbars (Lippmann et al., 2003). The shoreline has been observed to recede (prograde) more than 20 m landward (seaward) during growth (decay) of a storm. If these hot spots are owing to cross-shore sediment movement, transport between the swash and inner surf must be tremendous. Many previous studies of nearshore sediment transport have focused on the surf zone, partly because sediment transport in the thinner swash zone flows is complicated by interactions between surface- and bed-generated turbulence from, respectively,

*Corresponding author. Tel.: +1 352 392 9537x1439.
E-mail address: thsu@coastal.ufl.edu (T.-J. Hsu).

0278-4343/$ - see front matter
doi:10.1016/j.csr.2006.02.004

breaking waves and near-bed shear stress. However, sediment transport in the swash and inner-surf zones may be more important to rapid shoreline movement during storms.

In the surf zone, the offshore migration of sandbars has been attributed to mean offshore-directed flows (e.g., Thornton et al., 1996; Gallagher et al., 1998). In contrast, the response of sediment to unsteady wave forcing (Drake and Calantoni, 2001; Nielsen and Callaghan, 2003; Hsu and Hanes, 2004) and nonlinear wave boundary layer (BL) processes (Trowbridge and Young, 1989; Henderson et al., 2004) has been emphasized in predicting onshore bar migration (Elgar et al., 2001; Hoefel and Elgar, 2003; Henderson et al., 2004). However, the importance of these mechanisms to transport in the swash and inner-surf zones, where the bed sometimes is dry between waves and the breaking-wave turbulence may reach the bed owing to the shallow depths, is unknown.

Masselink and Hughes (1998) showed that different uprush and downrush friction coefficients are needed to model swash-zone transport using Bailard-type models (Bailard, 1981), presumably to account for physics not included in the quasi-steady (QS) parameterizations. Nielsen (2002) suggested a single friction coefficient could be used if terms were included in the sediment transport parameterization to account for flow accelerations resulting from skewed and asymmetric waves. Butt and Russell (1999) and Puleo et al. (2004) agree that flow accelerations are important, but suggest that the added terms are a proxy for enhanced transport resulting from turbulent suspension at the front face of the wave, where large accelerations coincide with intense bore turbulence (e.g., Osborne and Rooker, 1999; Puleo et al., 2000; Butt et al., 2004). Terms accounting for in- and exfiltration, which may alter the effective weight of sediment (e.g., Horn, 2002) and modify the BL structure and hence the bottom stress (Conley and Inman, 1994; Conley and Griffin, 2004), also have been included in models of swash sediment transport (Turner and Masselink, 1998; Butt et al., 2001).

Sediment transport is predominately driven by bottom BL shear flow. However, when the water depth in the swash or inner-surf zones becomes shallow relative to the broken-wave (or bore) height, the breaking-wave generated turbulence also may affect the near bed sediment transport, and the assumptions in existing boundary-layer-driven sediment transport parameterizations may not be valid.

Here, numerical models and field data are used to identify some of the small-scale processes that are important to sediment transport, and to justify simplifications that could enable larger-scale, longer-term simulations. In particular, the assumptions underlying the QS and power law approaches that phase lags between the transport, near-bed shear, and the flow forcing are negligible are examined.

In Section 2, mechanisms related to boundary-layer-shear-induced sediment transport are investigated by comparing predictions of a two-phase model (Hsu et al., 2004) and a (dilute) turbulent suspension model (Hsu and Liu, 2004) with two simplified approaches. In Section 3, turbulent fluctuations estimated from velocities measured between the shoreline and about 1-m water depth during the SwashX field experiment conducted in fall 2000 near La Jolla, CA (Raubenheimer, 2002) are examined to evaluate near-bed levels of breaking-wave-generated turbulence. In Section 4, assumptions that may be adopted to parameterize sediment transport and their limitations in the inner-surf and swash zones are discussed. The paper is concluded in Section 5.

2. Boundary-layer-shear-induced sediment transport

2.1. Method

Sediment transport is a continuous process across the BL involving particle intergranular interactions and fluid turbulent suspension. Detailed field measurements of these small-scale processes, especially in the concentrated region, are difficult to obtain. Models that calculate these processes can be computationally expensive, but also can provide information to improve parameterizations of sediment transport. Detailed two-phase (Hsu et al., 2004) and turbulent suspension (Hsu and Liu, 2004) models are used here to evaluate two simplified approaches.

Two-phase model: The two-phase model calculates the mass and momentum equations of both the fluid and sediment phases across the BL, including the most concentrated near-bed region. Closures for fluid turbulence and turbulent suspension are incorporated using eddy viscosity and k–ε equations, and closures for particle intergranular stresses are based on kinetic theory of collisional granular flow (Jenkins and Hanes, 1998). The sediment boundary condition at the instantaneous bed level is calculated using a modified Hertz contact relation and a failure condition, resulting in a bed concentration near that for random close packing (Hsu et al., 2004). In contrast to many other models, empirical parameterizations are not required for the bed roughness, a reference concentration (e.g., Hagatun and Eidsvik, 1986), or a pick-up function (e.g., van Rijn, 1984). Both the bottom stress (including contributions from both fluid and sediment stresses) and total transport rate are part of the solution of the model equations.

Turbulent suspension model: The turbulent suspension model used here (Hsu and Liu, 2004) falls in a broad category of suspended load models that assume sediment concentration is dilute and that use closures on fluid turbulence, particle fall velocity, and near-bed sediment boundary conditions (e.g., Hagatun and Eidsvik, 1986; Li and Davies, 1996; Henderson et al., 2004). The model calculates the fluid flow from the Reynolds-averaged Navier–Stokes equations using a k–ε turbulence closure. The suspended sediment concentration is calculated using an advection–diffusion equation (e.g., Nielsen, 1992). Unlike the two-phase model, the concentrated region of transport is not resolved, and therefore the model requires specification of an empirical bed roughness K_s (Sumer et al., 1996; Dohmen-Janssen et al., 2001) and a sediment pick-up function (van Rijn, 1984).

The models are driven with near-bed, cross-shore flow velocities measured during SwashX (Raubenheimer, 2002), and are used to predict the nondimensional instantaneous bottom stress

$$\theta(t) = \frac{\tau_b(t)}{\rho(s-1)gd}, \tag{1}$$

and the nondimensional sediment transport rate

$$\Psi(t) = \frac{q_b(t)}{\sqrt{(s-1)gd^3}}, \tag{2}$$

where $\tau_b(t)$ is the dimensional bottom stress, ρ is the fluid density, s is the specific gravity of the sediment, g is gravitational acceleration, d is the sediment grain diameter, and $q_b(t)$ is the dimensional sediment transport calculated by depth integrating the sediment horizontal flux obtained from the numerical models.

Simplified models: Bottom stresses and transport rates predicted by the detailed models are used to evaluate two simplified models, the QS model and the BL model. Both simplified models assume the time-dependent transport rate is in phase with the bottom stress and hence $\Psi(t)$ can be parameterized by $\theta(t)$ through a Meyer–Peter-type power law (e.g., Ribberink, 1998)

$$\Psi(t) = \frac{\theta(t)}{|\theta(t)|} C_0[|\theta(t)| - 0.05]^n, \tag{3}$$

where C_0 and n are free parameters that are adjusted to provide the best agreement with the detailed models.

The QS model calculates the time-dependent bottom stress from the wave forcing (demeaned free-stream velocity $\tilde{U}_0(t)$ above the wave boundary layer) using a quadratic law:

$$\tau_b = \frac{1}{2}\rho f_w \tilde{U}_0(t)|\tilde{U}_0(t)|, \tag{4}$$

where f_w is a wave friction factor. The QS model neglects boundary layer processes, such as the phase-lag between the free-stream velocity and the bottom stress.

On the other hand, the BL model calculates the BL fluid stresses (e.g., viscous and Reynolds stresses) using k–ε closure, and therefore incorporates wave boundary layer processes. Similar to the turbulent suspension model, the BL model does not calculate explicitly the intergranular and fluid–sediment interactions and requires specification of the roughness height K_s. However, unlike the turbulent suspension model, the BL model uses the power law (3) for the transport rate and assumes transport is in-phase with bottom stress.

The assumptions adopted by the simplified models, that the transport is in phase with the bottom stress (adopted by both QS and BL models) and that the bottom stress is in phase with the flow forcing (adopted by QS model), are examined next using the detailed models.

2.2. *Is the transport in phase with the bottom stress?*

The importance of phase lags between the transport and the bottom stress is investigated by comparing nondimensional sediment transport predicted directly by the detailed two-phase and turbulent suspension models with that predicted from the detailed model results of bottom stress time series and the Meyer–Peter-type power law (3). For coarse sand ($s = 2.65$, $d = 1.0$ mm) and sea-swell-dominated velocities (Figs. 1a–4a) measured in about 1-m water depth, the transport rate (Fig. 1c) predicted by the power law and bottom

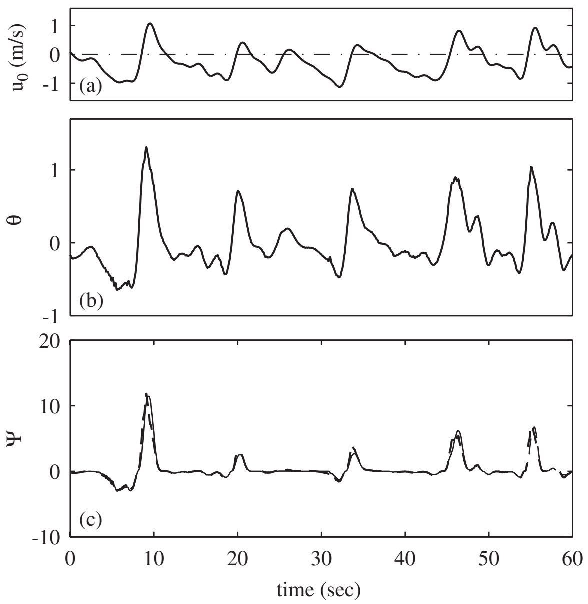

Fig. 1. (a) Observed sea-swell-dominated wave velocities, (b) corresponding nondimensional bottom stresses predicted by the two-phase model, and (c) nondimensional sediment transport predicted by the two-phase model (solid curve) and by the bottom stresses in (b) and the Meyer–Peter power law (dashed curve, $C_0 = 7.7$ and $n = 1.85$) for sand with $d = 1.0$ mm versus time.

stress (Fig. 1b) is correlated well (squared correlation $\gamma^2 = 0.92$) with that calculated by the two-phase model (compare dashed with solid curves in Fig. 1c).

Similarly, transport rates (Fig. 2b-2) for finer-grained sand ($d = 0.3$ mm) predicted by the turbulent suspension model ($K_s/d = 5.5$) and by the Meyer–Peter power law (using the bottom stresses predicted by the turbulent suspension model, Fig. 2b-1) are correlated well ($\gamma^2 = 0.85$, compare solid and dashed curves in Fig. 2b-2).

Agreement between the transport rate predicted by the detailed models and the power law decreases with decreasing grain size. For example, the correlation between the transport predicted by the turbulent suspension model and the power law decreases from $\gamma^2 = 0.85$ to 0.79 for decreasing $d =$ 0.3 to 0.2 mm (compare results shown in Figs. 2b-2 with those in 2c-2). For grain sizes $d = 0.13$ mm, the squared correlation is reduced further to 0.72 (not shown). For very small grain sizes, transport does not respond instantaneously to bottom stress owing to suspension high above the bed and to slow settling velocities, and thus the power law becomes inaccurate. However, for typical sandy-beach grain sizes (e.g., $0.2 \leqslant d \leqslant 0.5$ mm), the simulations suggest that transport is mostly in phase with the bottom stress, and the power law is an effective parameterization for the majority of the transport. At present, direct field (Conley and Griffin, 2004) or laboratory (e.g., Cowen et al., 2003) measurements of bottom stress remain difficult. Although the detailed model results shown here are limited by their closure assumptions, they provide justification for using the power law (3) (e.g., Ribberink, 1998) to parameterize the sediment transport rate.

Note that the choice of the roughness height K_s and the pick-up function used in the turbulent suspension model affects the best-fit values of the free parameters in the power law (C_0 and n). However, the conclusions that transport is in phase with the bottom stress for typical beach sands, and that discrepancies increase for decreasing grain size, are not affected.

2.3. *Is the bottom stress in phase with the flow forcing?*

The importance to sediment transport of phase lags between the bottom stress and the wave orbital velocities $\tilde{U}_0(t)$ is investigated by comparing nondimensional stresses predicted by the two-phase and turbulent suspension models with those predicted by the QS model (which neglects the phase lags) and BL model (which incorporates the phase lags through fluid turbulence), and by evaluating the effect on the predicted transport.

For sea-swell-dominated wave velocities (Figs. 3a and 4a) measured in about 1-m water depth and coarse sand ($s = 2.65$, $d = 1.0$ mm), the bottom stress predicted by the QS model is smaller under the passage of pitched-forward wave crests than the stress predicted by the two-phase model (compare dotted with solid curves in Fig. 3b, $\gamma^2 = 0.61$), resulting in significant underestimation of onshore sediment transport (compare dotted with solid curves in Fig. 3c, $\gamma^2 = 0.65$). Therefore, capturing the phase lag between the wave forcing and bottom stress may be important to swash- and inner-surf-zone sediment transport. Similar results are obtained for finer-grained sand ($d = 0.2$ mm) with transport simulated using the turbulent suspension and QS models (compare the solid curve with the dashed curve in Figs. 4b ($\gamma^2 = 0.70$) and 4c ($\gamma^2 = 0.55$)).

For infragravity-dominated wave velocities, the bottom stresses predicted by the turbulent suspension and QS models are better correlated (Fig. 5b,

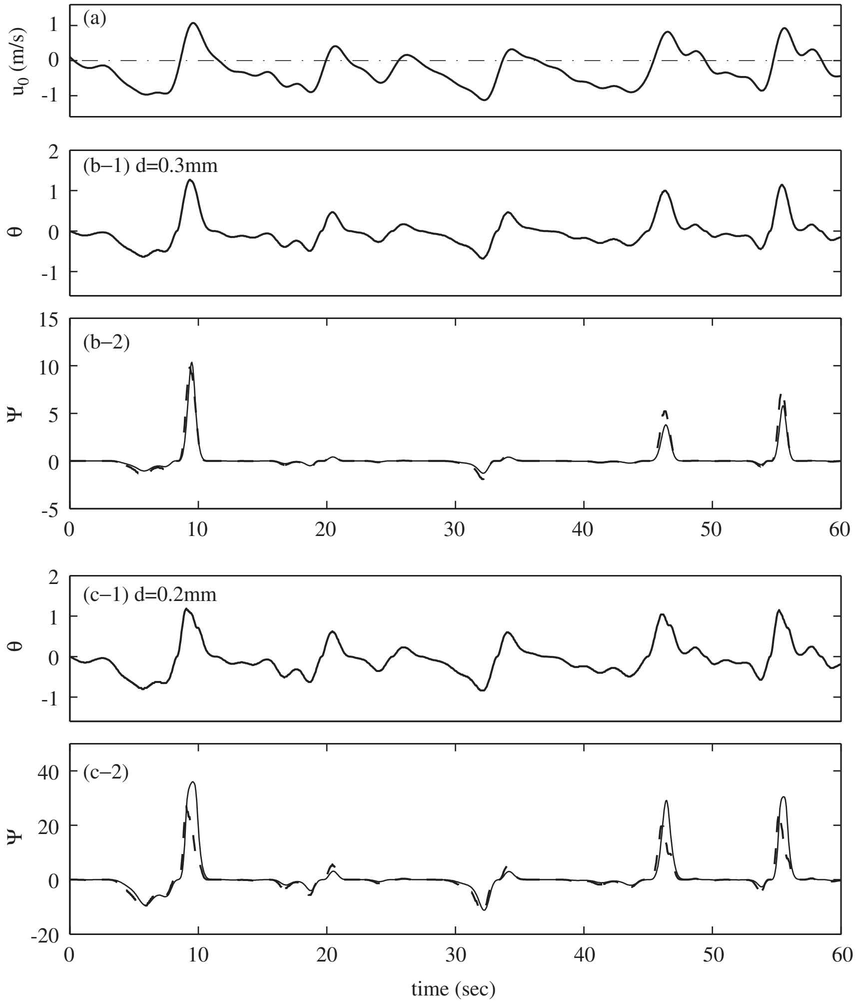

Fig. 2. (a) Observed sea-swell-dominated wave velocities and corresponding (b-1 and c-1) nondimensional bottom stresses and (b-2 and c-2) sediment transport for sediment with grain size (b-1 and b-2) $d = 0.3$ mm and (c-1 and c-2) $d = 0.2$ mm predicted by the turbulent suspension model (solid curve) and the Meyer–Peter power law (dashed curve) versus time. A roughness height of $K_s/d = 5.5$ (Sumer et al., 1996; Hsu and Liu, 2004) is used in the turbulent suspension model. The Meyer–Peter power law is driven with the stresses predicted by the turbulent suspension model with best fit parameters: $C_0 = 6.0,\ n = 2.5$ in b-2 and $C_0 = 18.0,\ n = 2.3$ in c-2.

compare solid curve with dashed curve, $\gamma^2 = 0.85$) than under sea-swell-dominated conditions (Fig. 4b, $\gamma^2 = 0.70$). Similarly, in contrast to sea-swell-dominated conditions, the transport rates predicted by the turbulent suspension model and by the power law (3) with stresses given by the QS model are highly correlated for infragravity-dominated conditions (Fig. 5c, compare solid curve with dashed curve, $\gamma^2 = 0.93$). For infragravity waves, the unsteadiness of the forcing (or acceleration) is smaller (even for saw-tooth-shaped waves), because the dominant wave period T is longer (e.g., $T = 10$ s for sea-swell waves (Fig. 4a) and 37 s for infragravity waves (Fig. 5a)). Thus, the QS approximation between the wave orbital velocities and the bottom stress is more applicable to infragravity-dominated than to sea-swell-dominated conditions. However, to ensure that onshore-directed transport is predicted well during all conditions, it is recommended that swash and inner-surf-zone transport models account for the phase lag between bottom stress and the flow forcing.

The stresses estimated by a BL (single-phase) model are similar to those predicted by the two-phase model (e.g., compare solid with dashed curves in Fig. 3b) if a large value is used for the roughness height $K_s/d = 35$. The roughness required in the single-phase approach, which is much larger than

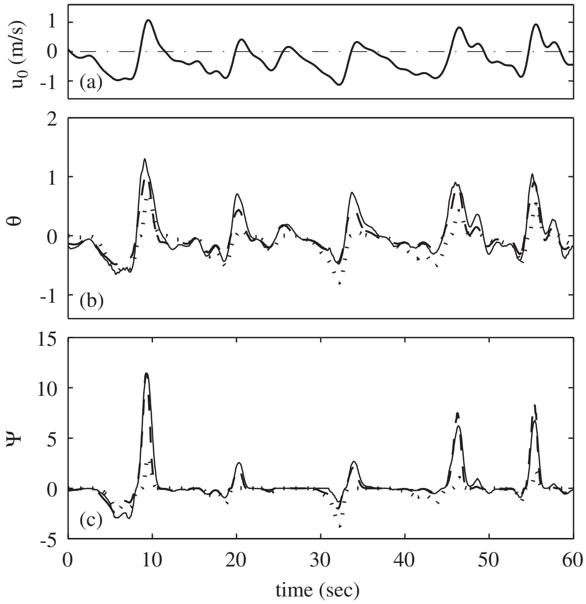

Fig. 3. (a) Observed sea-swell-dominated wave velocities, (b) corresponding nondimensional bottom stresses predicted by the two-phase model (solid curve), the single-phase boundary layer model (dashed curve, $K_s/d = 35$), and the QS model (dotted curve, $f_w = 0.0210$), and (c) nondimensional sediment transport predicted by the two-phase model (solid curve), and by the power law with bottom stress predicted by boundary layer (BL) model (dashed curve, $C_0 = 11.3$, $n = 1.85$) or by the QS model (dotted curve, $C_0 = 6.5$, $n = 1.85$) for coarse-grained sediment with $d = 1.0$ mm versus time.

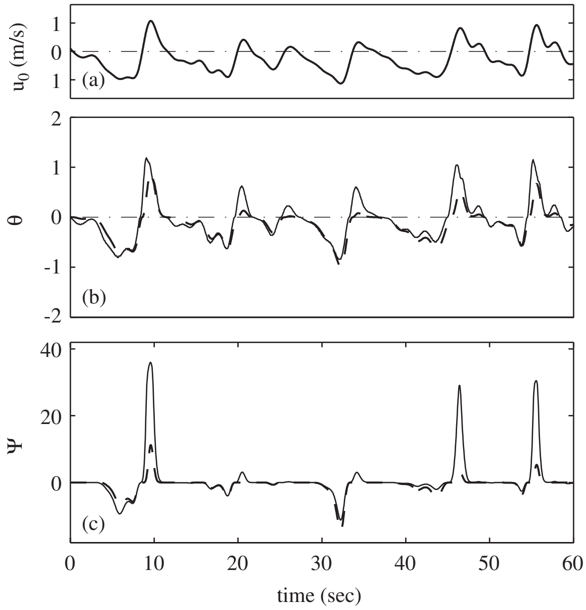

Fig. 4. (a) Observed sea-swell-dominated wave velocities, (b) corresponding nondimensional bed stresses predicted by the turbulent suspension model (solid curve, $K_s/d = 5.5$) and the QS model (dashed curve, $f_w = 0.0050$), and (c) nondimensional sediment transport predicted by the turbulent suspension model (solid curve) and by the power law model with stresses predicted by the QS model (dashed curve, $C_0 = 17.0$, $n = 2.40$) for fine-grained sediment with $d = 0.2$ mm versus time.

the typical value of $K_s \sim 2d$ for clear fluid flow, is supported by detailed measurement of sheet flow sediment transport in a U-tube (Dohmen-Janssen et al., 2001). The elevated roughness value is suspected to be a surrogate for energy dissipation by particle–particle and particle–fluid interactions. The optimal value of the roughness may depend on the wave conditions, the grain properties (e.g., size and density), and the viscosity of the interstitial fluid. Hence, for finer sand ($0.13 \leqslant d \leqslant 0.2$ mm), the roughness required by the turbulent suspension model is smaller $5 \leqslant K_s/d \leqslant 10$ (Sumer et al., 1996; Hsu and Liu, 2004).

3. Breaking-wave-generated turbulence

As the water depth becomes shallow in the inner-surf and swash zones, the breaking-wave-generated turbulence is hypothesized to influence the bottom BL and to affect sediment transport (e.g., Roelvink and Stive, 1989; Kobayashi and Johnson, 2001; Butt et al., 2004). This hypothesis is supported by field observations of high suspended sediment concentrations during passage of bore fronts or large flow accelerations (e.g., Hanes and Huntley, 1986; Hay and Bowen, 1994; Osborne and Rooker, 1999; Butt and Russell, 1999; Puleo et al., 2000; Butt et al., 2004). Recently, detailed U-tube and wave flume experiments have been used to show that breaking-wave-generated turbulence can influence the bottom BL flow structure and bottom stress (Cox and Kobayashi, 2000; Fredsøe et al., 2003; Cowen et al., 2003).

3.1. Field evidence

Consistent with near-bed parameterizations of bore-generated turbulence, high-frequency ($f > 1$ Hz) velocity fluctuations (assumed to represent turbulence) measured within a few cm above the bed during SwashX are significantly stronger during passage of the bore front (Fig. 6). During the initiation of onshore-directed flow in the swash zone (e.g. times $t \sim 25$ and 185 s), strong turbulent fluctuations are observed almost simultaneously (within $\sim$1 s) at both the highest (10 cm above the bed, Fig. 6b) and lowest (4 cm above bed, Fig. 6c)

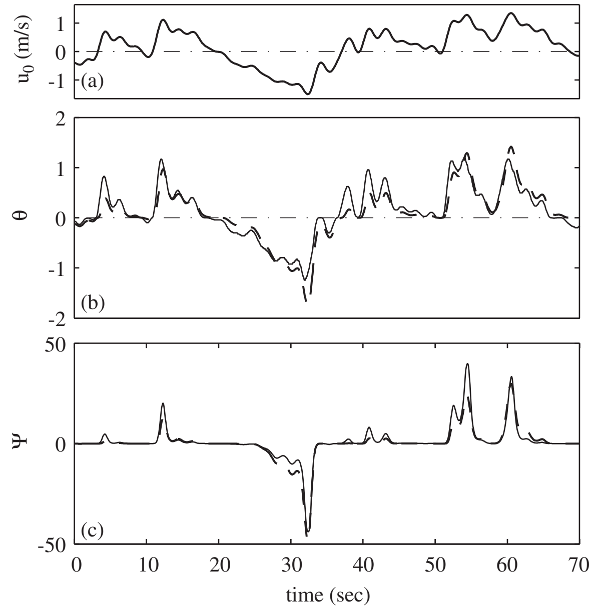

Fig. 5. (a) Observed infragravity-dominated wave velocities, (b) corresponding nondimensional bottom stresses predicted by the turbulent suspension model (solid curve, $K_s/d = 5.5$), and the QS model (dashed curve, $f_w = 0.0053$), and (c) nondimensional sediment transport predicted by the turbulent suspension model (solid curve), and by the power law (3) with stresses predicted by the QS model (dashed curve, $C_0 = 15.0$, $n = 2.20$) for fine-grained sediment with $d = 0.2$ mm versus time.

sensors, suggesting that surface-generated turbulence extends close to the bed. Note, the highest sensor requires deeper water than the lowest sensor before measuring flows. During an event ($t \sim 195$ s) in which a second wave overtakes the initial wave before the bed is exposed to air (e.g., the water depth is roughly 10 cm in front of the bore), strong turbulent fluctuations are observed only at the highest sensor (Fig. 6b), suggesting that in this event the turbulence generated by the bore did not reach the seabed.

The intensity of the nearbed breaking-wave-generated turbulence, quantified crudely as the ratio of the root-mean-square turbulent fluctuations (high-passed flows) to the wave velocities (low-passed flows), $\langle u'(t)\rangle/\langle u(t)\rangle$, is examined as a function of the normalized sensor depth $(D-r)/H$ (Trowbridge and Elgar, 2003), where D is the time-averaged water depth, r is the elevation of the sensor above the bed, and H is the root-mean-square sea surface fluctuation. The time-averaging window ranges from about 60 s in the inner surf zone to as little as 5 s in the upper-swash zone, depending on the period during which the bed is submerged (Fig. 7).

When $(D-r)/H > 2.5$ (typical for water depths greater than 40 cm), $\langle u'(t)\rangle/\langle u(t)\rangle$ is almost always less than 0.07 and the turbulent fluctuations are thought to be dominated by boundary-layer-generated turbulence. In contrast, $\langle u'(t)\rangle/\langle u(t)\rangle$ often is greater than 0.07 when $(D-r)/H < 2.5$ (typical of the swash zone). The frequently elevated near-bed turbulence presumably is owing to intermittent wave breaking (e.g., Fig. 6). Note that velocity sensors in swashes with $\langle u'(t)\rangle/\langle u(t)\rangle$ larger than 0.30 were submerged for not more than 10 s, and the estimated turbulence may not be reliable.

3.2. Discussion

The results suggest that surface-generated turbulence often will penetrate near the bed, and will affect sediment suspension and transport significantly for $(D-r)/H < 2.5$, which mostly corresponds to regions of the swash zone in which the bed is exposed between most waves (e.g., the upper- and mid-swash zones on low-sloped beaches and the entire swash zone on steep beaches). In contrast, bed-generated turbulence may dominate in water depths deeper than the outer swash. Thus, the numerical model study presented in Section 2, specifically the justification of the simplified model, may be applicable at least qualitatively in the outer swash and inner surf where mean water depths are greater than about 40 cm. More detailed understanding of the interactions between surface-generated turbulence and the bottom BL, and more importantly the effects on the resulting sediment transport, may be needed to model accurately sediment transport in the mid- and upper-swash zone.

Note that the low frequency cut-off used here (1 Hz) was chosen to fall within the inertial subrange determined by examining the energy spectrum (Raubenheimer et al., 2004), and to be consistent with similar field studies (e.g., Butt et al., 2004). However, it is expected that total turbulent energy is underestimated owing to neglect of low-frequency ($f \leqslant 1$ Hz) turbulent fluctuations resulting from large-scale coherent structures. In particular, regular wave data from a prototype-scale laboratory experiment (Scott et al., 2005) showed that the frequency filtering technique (cut-off frequency 1 Hz) underestimates turbulent fluctuations relative to a differencing technique (e.g., Trowbridge and

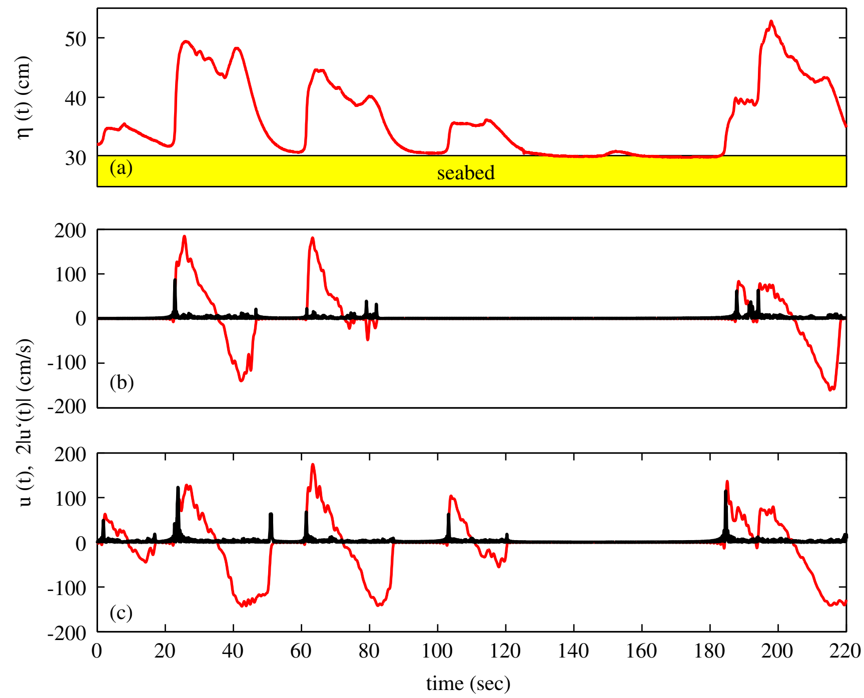

Fig. 6. (a) Observed swash-zone free-surface-elevation fluctuations, and (b and c) low-passed ($f \leqslant 1$ Hz, red solid curves) and two-times high-passed ($f > 1$ Hz, black solid curves) velocities measured (b) 10 and (c) 4 cm above the bed. Bed level is shown by the top of the solid yellow bar in (a). High-passed velocities (assumed to represent turbulent fluctuations) are shown at double magnitude to enable easy comparison with low-passed velocities.

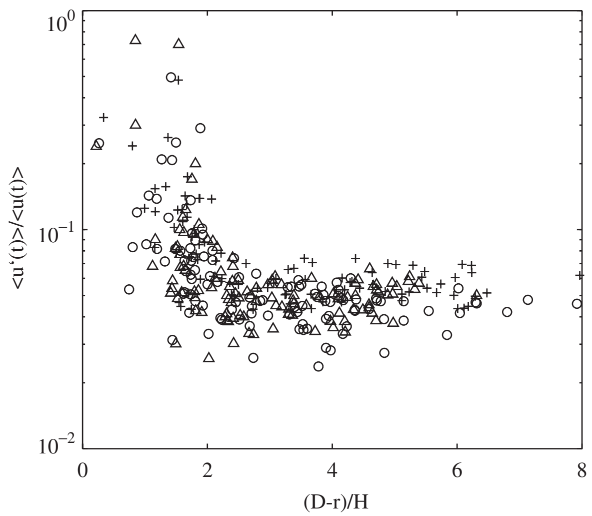

Fig. 7. Observed normalized near-bed turbulent intensity $\langle u'(t)\rangle/\langle u(t)\rangle$ versus normalized sensor depth $(D-r)/H$. Data were extracted from 51.2-min time series collected on September 28th 7 pm (pluses), September 29th 7 am (circles), and September 29th 8 pm (triangles).

Elgar, 2001) or to an ensemble (phase)-averaging technique. However, these more rigorous techniques are not possible with the SwashX data. In particular, the sensor separation precludes use of the differencing technique, which requires simultaneous measurement of velocities from two neighboring sensors located at a distance that is much larger than typical turbulent eddy size but close enough to neglect alongshore variations. Additionally, the random wave conditions on the natural beach preclude use of the ensemble averaging technique. However, the filtering technique provides a useful, conservative estimate of turbulent energy.

4. Conclusion

Field observations and numerical models are used to investigate small-scale processes important to boundary-layer-shear-induced sediment transport in the inner-surf and swash zones to guide parameterizations for a larger-scale, morphological-change model for sandy beaches. In particular, model simulations suggest that transport is in phase with the bottom stress, consistent with results in the outer-surf zone. However, the simulations suggest that phase lags between the bottom stress and the flow forcing are important to onshore sediment transport. Additionally, observations of high-frequency velocity fluctuations (assumed to represent turbulence) suggest that surface-generated turbulence at the breaking wave front penetrates through the water column to near the bed, affecting onshore-directed sediment transport in the swash zone.

Acknowledgments

Funding of this research is supported by Office of Naval Research (N00014-05-10082) and National Science Foundation (OCE-0095834, CTS-0426811). Woods Hole Oceanographic Institution contribution 11305.

References

Bailard, J.A., 1981. An energetics total load sediment transport model for a plane sloping beach. Journal of Geophysical Research 86, 10938–10954.

Butt, T., Russell, P., 1999. Suspended sediment transport mechanism in high energy swash. Marine Geology 161, 361–375.

Butt, T., Russell, P., Turner, I., 2001. The influence of swash infiltration–exfiltration on beach face sediment transport: onshore or offshore? Coastal Engineering 42, 35–52.

Butt, T., Russell, P., Puleo, J., Miles, J., Masselink, G., 2004. The influence of bore turbulence on sediment transport in the swash and inner surf zone. Continental Shelf Research 24, 757–771.

Cowen, E.A., Sou, I.M., Liu, P.L.-F., Raubenheimer, B., 2003. PIV measurements within a laboratory generated swash zone. Journal of Engineering Mechanics 120 (10), 1119–1129.

Conley, D., Griffin, J.G., 2004. Direct measurements of bed stress under swash in the field. Journal of Geophysical Research 109, C03050.

Conley, D., Inman, D.L., 1994. Ventilated oscillatory boundary layers. Journal of Fluid Mechanics 273, 262–284.

Cox, D.T., Kobayashi, N., 2000. Identification of intense, intermittent coherent motions under shoaling and breaking waves. Journal of Geophysical Research 105 (C6), 14223–14236.

Dohmen-Janssen, C.M., Hassan, W.N., Ribberink, J.S., 2001. Mobile-bed effects in oscillatory sheet flow. Journal of Geophysical Research 106 (C11), 27103–27115.

Drake, T.G., Calantoni, J., 2001. Discrete particle model for sheet flow sediment transport in the nearshore. Journal of Geophysical Research 106 (C9), 19859–19868.

Elgar, S., Gallagher, E.L., Guza, R.T., 2001. Nearshore sandbar migration. Journal of Geophysical Research 106 (C6), 11623–11627.

Fredsøe, J., Sumer, B.M., Kozakiewicz, A., Chua, L.H.C., Deigaard, R., 2003. Effect of externally generated turbulence on wave boundary layer. Coastal Engineering 49, 155–183.

Gallagher, E.L., Elgar, S., Guza, R.T., 1998. Observations of sand bar evolution on a natural beach. Journal of Geophysical Research 103 (C2), 3203–3215.

Hagatun, K., Eidsvik, K., 1986. Oscillating turbulent boundary layer with suspended sediments. Journal of Geophysical Research 91, 13045–13055.

Hanes, D.M., Huntley, D.A., 1986. Continuous measurements of suspended sand concentration in a wave dominated nearshore environment. Continental Shelf Research 6 (4), 585–596.

Hay, A.E., Bowen, A.J., 1994. On the spatial coherence scales of wave-induced suspended sand concentration fluctuations. Journal of Geophysical Research 99, 12749–12766.

Henderson, S.M., Allen, J.S., Newberger, P.A., 2004. Nearshore sandbar migration by an eddy-diffusive boundary layer model. Journal of Geophysical Research 109 (C6), C06024.

Hoefel, F., Elgar, S., 2003. Wave-induced sediment transport and sandbar migration. Science 299, 1885–1887.

Horn, D.P., 2002. Beach groundwater dynamics. Geomorphology 48 (1–3), 121–146.

Hsu, T.-J., Hanes, D.M., 2004. The effects of wave shape on coastal sheet flow sediment transport. Journal of Geophysical Research 109, C05025.

Hsu, T.-J., Liu, P.L.-F., 2004. Toward modeling sand suspension under waves. Journal of Geophysical Research 109 (C6), C06018.

Hsu, T.-J., Jenkins, J.T., Liu, P.L.-F., 2004. On two-phase sediment transport: sheet flow of massive particles. Proceedings of the Royal Society of London (A) 460 (2048), 2223–2250.

Jenkins, J.T., Hanes, D.M., 1998. Collisional sheet flows of sediment driven by turbulent fluid. Journal of Fluid Mechanics 370, 29–52.

Kobayashi, N., Johnson, B.D., 2001. Sand suspension, storage, advection, and settling in surf and swash zones. Journal of Geophysical Research 106 (C5), 9363–9376.

Li, Z., Davies, A.G., 1996. Toward predicting sediment transport in combined wave-current flow. Journal of Waterway Port Coastal and Ocean Engineering 122, 157–164.

Lippmann, T.C., List, J.H., Kannan, S. 2003. Shoreline response to storms and the configuration of nearshore sand bars. Proceedings of the 28th International Conference on Coastal Engineering, ASCE.

List, J.H., Farris, A.S., 1999. Large-scale shoreline response to storms and fair weather. Proceedings of the Coastal Sediments' 00, ASCE, Reston, VA, pp. 1324–1338.

List, J.H., Birkemeier, W.A., Ruggiero, P., Long, C.E., 2003. An experiment on the large-scale coastal response to storms. Eos Transactions of AGU 84(52), Ocean Science Meeting Supplement, Abstract OS32F-07.

Masselink, G., Hughes, M., 1998. Field investigation of sediment transport in the swash zone. Continental Shelf Research 18, 1179–1199.

Nielsen, P., 1992. Coastal Bottom Boundary Layers and Sediment Transport. World Scientific, Singapore.

Nielsen, P., 2002. Shear stress and sediment transport calculations for swash zone modelling. Coastal Engineering 45, 53–60.

Nielsen, P., Callaghan, D.P., 2003. Shear stress and sediment transport calculations for sheet flow under waves. Coastal Engineering 47, 347–354.

Osborne, P.D., Rooker, G.A., 1999. Sand re-suspension events in a high energy infragravity swash zone. Journal of Coastal Research 15 (1), 74–86.

Puleo, J.A., Beach, R.A., Holman, R.A., Allen, J.S., 2000. Swash zone sediment suspension and transport and the importance of bore-generated turbulence. Journal of Geophysical Research 105 (C7), 17021–17044.

Puleo, J.A., Holland, K.T., Plant, N.G., Slinn, D.N., Hanes, D.M., 2004. Fluid acceleration effects on suspended sediment transport in the swash zone. Journal of Geophysical Research 108 (C11), 3350.

Raubenheimer, B., 2002. Observations and predictions of fluid velocities in the surf and swash zones. Journal of Geophysical Research 107 (C11), 3190.

Raubenheimer, B., Elgar, S., Guza, R.T., 2004. Observations of swash zone velocities a note on friction coefficients. Journal of Geophysical Research 109, C01027.

Ribberink, J.S., 1998. Bed-load transport for steady flows and unsteady oscillatory flows. Coastal Engineering 34, 59–82.

Roelvink, J.A., Stive, M.J.F., 1989. Bar generating cross-shore flow mechanisms on a beach. Journal of Geophysical Research 94, 4785–4800.

Scott, C.P., Cox, D.T., Maddux, T.B., Long, J.W., 2005. Large-scale laboratory observations of turbulence on a fixed barred beach. Measurement Science and Technology 16 (10), 1903–1912.

Sumer, B.M., Kozakiewicz, A., Fredsøe, J., Deigaard, R., 1996. Velocity and concentration profiles in sheet-flow layer of movable bed. Journal of Hydraulic Engineering 122, 549–558.

Thornton, E., Humiston, R., Birkemeier, W., 1996. Bar-trough generation on a natural beach. Journal of Geophysical Research 101, 12097–12110.

Trowbridge, J., Elgar, S., 2003. Spatial scales of stress-carrying nearshore turbulence. Journal of Physical Oceanography 33, 1122–1128.

Trowbridge, J., Young, D., 1989. Sand transport by unbroken waves under sheet flow conditions. Journal of Geophysical Research 94, 10971–10991.

Turner, I.L., Masselink, G., 1998. Swash infiltration–exfiltration and sediment transport. Journal of Geophysical Research 103 (C13), 30813–30824.

van Rijn, L.C., 1984. Sediment pick-up function. Journal of Hydraulic Engineering 110 (10), 1494–1502.